

# JAAS

Accepted Manuscript



This is an *Accepted Manuscript*, which has been through the Royal Society of Chemistry peer review process and has been accepted for publication.

*Accepted Manuscripts* are published online shortly after acceptance, before technical editing, formatting and proof reading. Using this free service, authors can make their results available to the community, in citable form, before we publish the edited article. We will replace this *Accepted Manuscript* with the edited and formatted *Advance Article* as soon as it is available.

You can find more information about *Accepted Manuscripts* in the [Information for Authors](#).

Please note that technical editing may introduce minor changes to the text and/or graphics, which may alter content. The journal's standard [Terms & Conditions](#) and the [Ethical guidelines](#) still apply. In no event shall the Royal Society of Chemistry be held responsible for any errors or omissions in this *Accepted Manuscript* or any consequences arising from the use of any information it contains.

# Lead isotopic analysis of Antarctic snow using multi-collector ICP-mass spectrometry

Andrea Bazzano<sup>1,2</sup>, Kris Latruwe<sup>2</sup>, Marco Grotti<sup>1</sup>, Frank Vanhaecke<sup>2</sup>

<sup>1</sup>Department of Chemistry and Industrial Chemistry, University of Genoa, Via Dodecaneso 31, 16146 Genoa, Italy.

<sup>2</sup>Department of Analytical Chemistry, Ghent University, Krijgslaan 281-S12, 9000 Ghent, Belgium.

## Abstract

Reliable determination of Pb isotope ratios in Antarctic snow is challenging because of the low analyte concentration and the low volume of sample typically available. In this work, a combination of a total sample consumption introduction system (the torch-integrated sample introduction system, TISIS) with multi-collector ICP-mass spectrometry (MC-ICP-MS) was used for this purpose. With this instrumental setup, accurate and precise determination of Pb isotope ratios was possible at concentrations as low as  $0.5 \text{ ng mL}^{-1}$ , while using 0.2 mL of solution only (total amount of Pb: 100 pg). At  $10 \text{ ng mL}^{-1}$ , the repeatability for the  $^{207}\text{Pb}/^{206}\text{Pb}$  ratio was 0.16 % RSD. The concentration range was further extended downwards by using 100-fold analyte element preconcentration via freeze-drying of 20 g of snow. The Pb concentration in procedural blanks was  $0.5 \pm 0.3 \text{ pg g}^{-1}$ , enabling the determination of Pb isotope ratios in snow samples containing down to  $5 \text{ pg g}^{-1}$  of Pb. After development and validation, the procedure was applied to snow samples collected at Dome C (East Antarctic Plateau) on a monthly basis during the 2006 and 2010 campaigns. The method developed was able to reveal a seasonal variation in the Pb isotope ratios occurring during 2006 and strong inter-annual variation between the two campaigns.

## 1. Introduction

The determination of Pb isotope ratios in the Antarctic and Greenland snow and ice caps can provide valuable information on the geographical sources of both natural and anthropogenic atmospheric inputs, the relative contributions of these sources over time and the corresponding transport routes.<sup>1-3</sup> The accurate measurement of these isotope ratios can, however, be quite challenging. Indeed, the Pb concentration in polar snow and ice is extremely low, typically at or below the  $\text{pg g}^{-1}$  level,<sup>4</sup> therefore requiring the application of ultraclean procedures for sampling, sample storage and treatment, as well as very high instrument sensitivities.

Isotope dilution-thermal ionisation mass spectrometry (ID-TIMS) is capable of the simultaneous determination of the concentration of Pb and its isotopic composition and therefore appears to be the method of choice for the analysis of snow and ice samples of limited size.<sup>5,6</sup> Multi-collector inductively coupled plasma-mass spectrometry (MC-ICP-MS) can be considered a strong competitor of TIMS for many applications,<sup>7</sup> but so far, it has not been employed for the determination of Pb isotope ratios in snow samples from polar areas. For achieving an adequate isotope ratio precision, a relatively high target element concentration is required due to the low analyte transport efficiency from the sample solution to the detectors and the modest sensitivity of the Faraday cups used for ion monitoring. For many sample types, this problem can be circumvented via an analyte pre-concentration step, but this approach requires relatively large sample amounts, thus reducing the spatial/temporal resolution of the information provided in the specific case of Pb isotopic analysis of snow samples. A way to increase the instrument sensitivity, while adhering to a low sample consumption, is the use of a so-called “total consumption” sample introduction system. Among these total consumption devices, the torch integrated sample introduction system (TISIS)<sup>8,9</sup> was already proven capable of efficient introduction of microsamples into an ICP source, in both atomic emission (ICP-AES)<sup>10,11</sup> and mass spectrometry (ICP-MS).<sup>12,13</sup> In its final design, the TISIS consists of a single-pass high-temperature evaporation chamber, with a

1  
2 48 lateral port to introduce a sheathing gas stream, in a location close to the aerosol production point.  
3  
4 49 In this way, the aerosol solvent evaporation was enhanced and the impact of droplets against the  
5  
6 50 cavity walls reduced.  
7  
8  
9 51 Paredes *et al.* investigated the performance of a TISIS coupled with MC-ICP-MS for the  
10  
11 52 determination of Pb<sup>14</sup> and Sr<sup>15,16</sup> isotope ratios. Accurate data were obtained at a very low sample  
12  
13 53 uptake rate (5 – 30  $\mu\text{L min}^{-1}$ ) and at a total sample consumption of less than 0.3 mL of solution.  
14  
15 54 However, in these works, relatively high element concentrations were considered, resulting in a  
16  
17 55 signal strength of about 1 V for the most abundant isotope monitored. The low concentration levels  
18  
19 56 of Pb in snow from remote areas brings us far away from these ideal conditions.  
20  
21  
22 57 In this work, snow samples were first submitted to analyte pre-concentration, based on sample  
23  
24 58 volume reduction by freeze-drying.<sup>17</sup> The solutions thus obtained were introduced into an MC-ICP-  
25  
26 59 MS instrument for Pb isotopic analysis using a TISIS. This analytical protocol was optimised,  
27  
28 60 characterised in terms of precision and accuracy at ultra-trace concentration level, and, finally,  
29  
30 61 applied to the analysis of recent snow collected from Antarctica during two year-round expeditions.  
31  
32  
33  
34

## 35 62 **2. Materials and methods**

36  
37  
38 63 All solutions were prepared with ultrapure water (resistivity  $\geq 18.2 \text{ M}\Omega \text{ cm}$ ), obtained from a Milli-  
39  
40 64 Q Element water purification system (Millipore, Molsheim, France). Suprapur® 65 % HNO<sub>3</sub> from  
41  
42 65 Merck (Darmstadt, Germany) was used for the cleaning of materials, while Trace Select® Ultra 65  
43  
44 66 % HNO<sub>3</sub> from Sigma-Aldrich (St. Louis, MO, USA) was used for the final stage of the cleaning  
45  
46 67 procedure. Optima™ HNO<sub>3</sub> from Fisher Chemicals (Waltham, MA, USA) was used for the  
47  
48 68 preparation of standards and samples.  
49  
50

51  
52 69 All work, except for the pre-concentration procedure, was carried out in a metal-free class-10 clean  
53  
54 70 lab facility at Ghent University. The pre-concentration procedure was accomplished in a class-100  
55  
56 71 laminar flow area at the University of Genoa.  
57  
58

## 2.1. Standard reference materials

Isotopic reference materials for Pb (NIST SRM 981) and Tl (NIST SRM 997), acquired from the National Institute for Standards and technology (NIST, Gaithersburg, MD, USA), were used for correction for the bias introduced by instrumental mass discrimination. A solution containing 10 ng mL<sup>-1</sup> of both elements in 0.05 % ultrapure HNO<sub>3</sub> matrix was prepared for that purpose. The values used for the mass bias correction were  $^{207}\text{Pb}/^{206}\text{Pb} = 0.91464 \pm 0.00033$ ;  $^{208}\text{Pb}/^{206}\text{Pb} = 2.1681 \pm 0.0008$ ;  $^{208}\text{Pb}/^{207}\text{Pb} = 2.3704 \pm 0.00049$  and  $^{203}\text{Tl}/^{205}\text{Tl} = 0.418922 \pm 0.00028$ , as reported on the certificates released by the NIST.

A 10 ng mL<sup>-1</sup> in-house isotopic standard was prepared by serial dilution of a commercially available 1 mg mL<sup>-1</sup> stock solution (Inorganic Ventures, Christiansburg, VA, USA; lot G2-PB03044) and is further referred to as “A&MS-Pb”. Lead isotope ratios for this solution are  $^{207}\text{Pb}/^{206}\text{Pb} = 0.90413 \pm 0.00002$ ,  $^{208}\text{Pb}/^{206}\text{Pb} = 2.15331 \pm 0.00003$  and  $^{208}\text{Pb}/^{207}\text{Pb} = 2.38167 \pm 0.00003$  (average  $\pm$  95 % confidence interval;  $n = 15$ ; determined at 100 ng Pb mL<sup>-1</sup> using a conventional sample introduction system working at sample uptake rate of 200  $\mu\text{L min}^{-1}$ ).

## 2.2. Instrumentation and measurements

Lead isotope ratios were measured using a Thermo Scientific (Bremen, Germany) Neptune MC-ICP-MS instrument, operating at low mass resolution. The solutions were introduced into the plasma by means of a PFA nebuliser, operating in self-aspiration mode at a flow rate of 20  $\mu\text{L min}^{-1}$ , mounted onto the TISIS chamber. The system required 0.2 mL of solution for each analysis. The instrument settings and data acquisition parameters are summarized in Table 1.

All sample and standard solutions were prepared in 0.05 % ultrapure HNO<sub>3</sub> doped with 10 ng mL<sup>-1</sup> of Tl (NIST SRM 997) and the correction for the bias introduced by instrumental mass discrimination was performed offline using the method proposed by Woodhead *et al.*<sup>18</sup> and further refined by Baxter *et al.*<sup>19</sup>. With this method, a regression line in ln-ln space is determined by measuring both the isotope ratio for Tl (NIST SRM 997) and that selected for Pb (NIST SRM 981)

1  
2 97 in a series of standard solutions. Based on the regression line thus obtained and the Tl isotope ratio  
3  
4 98 measured for NIST SRM 997 Tl, admixed to the sample, the mass bias is corrected for.

5  
6 99 The A&MS-Pb solution was analysed as a quality control sample every five samples, whereas a full  
7  
8  
9 100 procedural blank was analysed for every analytical batch.

### 101 2.3. *Sample collection and analysis*

102 Antarctic snow samples were collected with a monthly resolution at Dome C (East Antarctic  
103 Plateau) during the 2006 and 2010 campaigns. In order to prevent contamination during sampling,  
104 the scientists taking the samples wore a clean room suit and approached the sampling site upwind.  
105 The samples were collected in acid-cleaned 50 mL PP graduated tubes (Kartell, Milan, Italy), sealed  
106 inside double polyethylene bags and stored at -20 °C until analysis. Following a previously  
107 developed procedure,<sup>20</sup> samples were first allowed to melt in their closed tubes. Subsequently, 20 g  
108 aliquots were transferred into acid-cleaned 50 mL PP graduated tubes, acidified with 100 µL of  
109 HNO<sub>3</sub> and refrozen. Then, the samples were freeze-dried, re-dissolved in 0.2 mL of 0.05 % HNO<sub>3</sub>  
110 solution containing 10 ng mL<sup>-1</sup> of Tl (NIST SRM 997) and analysed using MC-ICP-MS.

## 111 3. Results and discussion

### 112 3.1. *Sensitivity and stability of the signal*

113 Instrumental sensitivity strongly depended on the combination of both nebuliser and sheathing gas  
114 flow rate, resulting in a behaviour similar to that described earlier for different instrument set-  
115 ups.<sup>12,15</sup> Under optimum conditions, 10 ng mL<sup>-1</sup> of Pb (NIST SRM 981) gave rise to a signal of  
116 about 0.4 V for <sup>208</sup>Pb with a variation < 2 % RSD over a period of more than six hours of analysis.

117 The signal produced by the reagents blank (0.05 % of ultrapure HNO<sub>3</sub>) was about 10<sup>-5</sup> V for <sup>208</sup>Pb  
118 and was stable during approximately six hours of analysis. After this period of time, signal spikes  
119 usually started to appear, necessitating the analysis to be stopped. In such an event, the TISIS

1  
2  
3  
4  
5  
6  
7  
8  
9  
10  
11  
12  
13  
14  
15  
16  
17  
18  
19  
20  
21  
22  
23  
24  
25  
26  
27  
28  
29  
30  
31  
32  
33  
34  
35  
36  
37  
38  
39  
40  
41  
42  
43  
44  
45  
46  
47  
48  
49  
50  
51  
52  
53  
54  
55  
56  
57  
58  
59  
60

120 chamber was thoroughly cleaned by immersion in a bath of hot HNO<sub>3</sub> (about 10 % v/v) for several  
121 hours. This phenomenon was already described by Paredes *et al.*<sup>14</sup> and is likely due to the re-  
122 nebulisation of dry analyte particles from the nebuliser tip and the spray chamber walls.

### 123 3.2. Precision and repeatability

124 Precision is an important parameter for all analytical methods dealing with the measurement of  
125 isotope ratios, since it directly influences the uncertainties associated to each value, and thus, the  
126 capability to obtain a meaningful interpretation of the results.

127 The repeatability or internal precision (RSD for 42 successive measurements) was studied in a  
128 concentration range from 0.5 to 10 ng mL<sup>-1</sup> of Pb (NIST SRM 981), equivalent to a total Pb amount  
129 from 0.1 to 2 ng. In Figure 1, the RSD for the <sup>207</sup>Pb/<sup>206</sup>Pb ratio is reported, showing values below  
130 1.5 ‰ in the entire concentration range studied. At 10 ng mL<sup>-1</sup> of Pb, the RSD was 0.16 ± 0.03 ‰  
131 (average ± 95 % confidence interval). This value is more than an order of magnitude better than that  
132 reported using the same sample introduction system, but using a quadrupole-based ICP-MS  
133 instrument with ammonia as a damping gas for smoothing the fluctuations of the ion beam intensity  
134 for Pb isotope ratio measurements.<sup>17</sup>

135 The intermediate or external precision was assessed by measuring the <sup>207</sup>Pb/<sup>206</sup>Pb ratio in a solution  
136 with 10 ng mL<sup>-1</sup> of Pb (NIST SRM 981) over a period of more than three months and was 0.11 ‰  
137 (0.91465 ± 0.00005, *n* = 73) when expressed as twice the relative standard deviation of the ratios  
138 (not the standard error of the mean). This result is very similar to that obtained by Cocherie *et al.*,<sup>21</sup>  
139 who reported a value of 0.1 ‰ using a similar MC-ICP-MS instrument and a sample uptake rate of  
140 50 μL min<sup>-1</sup>. Similar values have also been reported by Kuritani *et al.*<sup>22</sup> (0.13 ‰) and Amelin *et*  
141 *al.*<sup>23</sup> (0.07 ‰) for isotopic analysis of absolute amounts of Pb of 1 and 2 ng by TIMS and double-  
142 spike TIMS, respectively. On the other hand, Makishima *et al.*<sup>24</sup> reported a reproducibility down to  
143 0.03 ‰ in the isotopic analysis of 1 ng of Pb at a sample uptake rate of 50 μL min<sup>-1</sup> (0.2 mL total  
144 sample consumption) when using an Aridus II aerosol desolvation system and a Neptune MC-ICP-

1  
2 145 MS instrument equipped with a Jet-type skimmer cone (also termed X-type), characterised by  
3  
4 146 enhanced transport efficiency. Finally, Thirlwall<sup>25</sup> reported an external precision of 0.06–0.18 ‰ (2  
5  
6 147 SD) for isotopic analysis of ~7 ng of Pb using double-spike MC-ICP-MS and the Aridus  
7  
8 148 desolvation system.

9  
10 149 When reducing the Pb concentration to 0.5 ng mL<sup>-1</sup>, the intermediate precision deteriorated to 0.31  
11  
12 150 ‰ (0.91438 ± 0.00028, *n* = 3) for the <sup>207</sup>Pb/<sup>206</sup>Pb ratio.

### 151 3.3. Validation of the measurement results

152 The validity of the Pb isotope ratios determined via the newly developed method was evaluated by  
153 analysing the in-house A&MS-Pb standard, previously characterized using the standard MC-ICP-  
154 MS procedure. The average biases and their accompanying 95 % confidence intervals for  
155 <sup>207</sup>Pb/<sup>206</sup>Pb measurement were 0.06 ± 0.03 ‰ (*n* = 25) and 0.25 ± 0.08 ‰ (*n* = 3) at 10 and 0.5 ng  
156 mL<sup>-1</sup>, respectively. The reported biases are within the range defined by the intermediate precision  
157 calculated in the previous section, thus the method provides accurate lead isotope ratios over the  
158 range of Pb concentration from 0.5 to 10 ng mL<sup>-1</sup>.

### 159 3.4. Procedural blanks

160 The instrumental performance reported on so far deemed suitable for the accurate determination of  
161 <sup>207</sup>Pb/<sup>206</sup>Pb, <sup>208</sup>Pb/<sup>206</sup>Pb and <sup>208</sup>Pb/<sup>207</sup>Pb ratios at concentration levels from 0.5 to 10 ng mL<sup>-1</sup>, using  
162 0.2 mL of solution only and therefore, requiring 0.1 to 2 ng of total Pb only. In order to further  
163 decrease the lowest concentration feasible, a simple pre-concentration procedure relying on freeze-  
164 drying was used for sample pre-treatment. The corresponding blank contribution was estimated on  
165 the basis of 5 synthetic samples, obtained by pouring 20 g of ultrapure water (the same mass as for  
166 the snow samples) in acid-cleaned tubes that were subsequently submitted to the entire analytical  
167 procedure.

1  
2  
3  
4  
5  
6  
7  
8  
9  
10  
11  
12  
13  
14  
15  
16  
17  
18  
19  
20  
21  
22  
23  
24  
25  
26  
27  
28  
29  
30  
31  
32  
33  
34  
35  
36  
37  
38  
39  
40  
41  
42  
43  
44  
45  
46  
47  
48  
49  
50  
51  
52  
53  
54  
55  
56  
57  
58  
59  
60

168 The Pb concentration was estimated by comparing the Pb intensity observed for the blanks to that of  
169 the closest standards (NIST SRM 981 at 10 ng mL<sup>-1</sup>), resulting in a concentration of 0.5 ± 0.3 pg g<sup>-1</sup>  
170 (or an absolute amount of 10 ± 6 pg Pb) and a Pb isotopic composition characterized by <sup>207</sup>Pb/<sup>206</sup>Pb  
171 = 0.868 ± 0.008 and <sup>208</sup>Pb/<sup>206</sup>Pb = 2.103 ± 0.020. Taking these results into account, the blank can  
172 induce variations in the isotopic composition ranging from 0.1 to 0.2% in snow samples with a Pb  
173 concentration of 5 pg g<sup>-1</sup>, the lowest Pb concentration encountered in the snow samples analyzed. A  
174 bias of this magnitude is relatively small compared to the natural variation in the isotopic  
175 composition of Pb as measured in Antarctic snow and ice.<sup>2,26</sup>

### 176 3.5. Uncertainty estimation

177 In order to discriminate different isotope ratios and hence, apply the results of isotopic analysis to  
178 environmental studies, a realistic estimation of the uncertainty is needed. The total uncertainty was  
179 calculated by combining the different single contributions, according to the GUM guidelines.<sup>27</sup> The  
180 contributions considered are related to (i) the instrumental precision in measuring the Pb isotope  
181 ratios in the samples ( $r_x$ ), (ii) the precision in measuring the Tl isotope ratio ( $r_s$ ), (iii) the error  
182 associated to the reference values for NIST SRM 981 ( $R_c$ ), and (iv) the error due to the blank  
183 subtraction ( $r_b$ ).

184 The relative contributions for the first three effects were estimated and propagated according to  
185 equation (2), previously reported by Baxter *et al.*<sup>19</sup> (supplementary material), and based on the  
186 assumption that the input quantities are not correlated

$$187 \frac{u_c^2(R_{x,\text{corr}})}{R_{x,\text{corr}}^2} = \frac{s_m^2(r_x)}{r_x^2} + \frac{s_m^2(r_s)}{r_s^2} [b^2 + s_m^2(b)] \left[ \ln \left( \frac{r_s}{\rho_{s,\text{SRM}}} \right) \right]^2 + \frac{s_m^2(R_c)}{R_c^2} \quad (2)$$

188 Here  $b$  is the estimated slope of the regression line used for the mass-bias correction,  $\rho$  denotes the  
189 means of the uncorrected ratios for the analyte and  $s_m^2(r_i)$  is the standard error of the mean for a  
190 generic ratio  $r_i$  measured within the blocks. Due to the low influence of  $s_m^2(b)$  (< 1% of the total  
191 uncertainty budget), it was merged with  $s_m^2(r_s)$ .

192 The relative contribution from the blank was estimated as the difference in the combined  
193 uncertainty calculated before and after the subtraction of the intensity of the blank.

194 Finally, the expanded uncertainty was calculated by multiplying the combined uncertainty,  $u_c(R_{x,corr})$   
195 with a coverage factor  $k = 2$ .

196 In figure 2, the different contributions to the combined uncertainty are visualized at concentrations  
197 of 5, 23 and 700  $\text{pg g}^{-1}$ , corresponding to the minimum, median and maximum concentration found  
198 in the Antarctic snow samples analysed (see next section). In the first case, the major contributions  
199 came from the instrumental precision (57 %) and the blank (37 %), whereas the contribution from  
200 the uncertainty on the NIST SRM 981 certified value accounted for 6 % only. On the other hand, at  
201 higher concentrations, 55 – 77 % of the uncertainty is attributed to the uncertainty of the certified  
202 value, 20 – 41 % is stemming from the Pb isotope ratio measurement precision, while the  
203 contribution to the uncertainty coming from the blank is lower than 2 %.

204 Despite the increased influence of the blank at low concentrations, it did not appear to be the main  
205 effect in the range of concentrations from 5 to 700  $\text{pg g}^{-1}$ . The contribution from the uncertainty on  
206 the certified value was found to become dominant at concentrations above 20  $\text{pg g}^{-1}$ . A better  
207 precision can be achieved when using the literature data obtained for NIST SRM 981 by double  
208 spike techniques<sup>24,25,28,29</sup> instead of the NIST certified values, but it could be argued that the  
209 confidence in these data cannot be as high as in the certified values. At Pb concentrations below 20  
210  $\text{pg g}^{-1}$ , the uncertainty associated to the Pb isotope ratios can be reduced by up to 40 % by  
211 increasing the instrument sensitivity. Additionally, lowering the blank level could result in reducing  
212 the uncertainty by more than 20 % for samples with Pb concentrations below 10  $\text{pg g}^{-1}$ .

### 213 3.6. *Lead isotope ratios measured in recent Antarctic snow with monthly resolution*

214  $^{207}\text{Pb}/^{206}\text{Pb}$ ,  $^{208}\text{Pb}/^{206}\text{Pb}$  and  $^{208}\text{Pb}/^{207}\text{Pb}$  isotopes ratios were determined in recent snow samples,  
215 collected on a monthly basis during the 2006 and 2010 campaigns. Snow from inland Antarctica is a  
216 very simple matrix, not requiring any Pb isolation step. Indeed the most abundant specie is  $\text{Na}^+$ , the

1  
2 217 concentration of which is typically below  $100 \text{ ng mL}^{-1}$ .<sup>30,31</sup> Therefore, the  $\text{Na}^+$  concentration after  
3  
4 218 the sample preparation step ( $< 10 \text{ } \mu\text{g mL}^{-1}$ ) was well below the concentration ( $400 \text{ } \mu\text{g mL}^{-1}$ ) for  
5  
6 219 which Cocherie *et al.*<sup>21</sup> reported a 0.09 ‰ bias in the MC-ICP-MS  $^{207}\text{Pb}/^{206}\text{Pb}$  measurement.

7  
8 220 The analytical procedure required 20 g of snow and about 10 minutes for each isotope ratio  
9  
10 221 measurement. The Pb concentration was estimated by comparison of the Pb intensity observed for  
11  
12 222 the sample to that of the closest standards (NIST SRM 981 at  $10 \text{ ng mL}^{-1}$ ) and it ranged from 5 to  
13  
14 223  $707 \text{ pg g}^{-1}$  (0.1 to  $14.1 \text{ ng of Pb}$ ), with a median value of  $23 \text{ pg g}^{-1}$  (0.5 ng of Pb). The estimated Pb  
15  
16 224 amount, the ratios obtained and their uncertainties (95 % confidence interval) are reported in Table  
17  
18 225 2.

19  
20  
21 226 At  $5 \text{ pg g}^{-1}$  Pb concentration, the uncertainty on the  $^{207}\text{Pb}/^{206}\text{Pb}$  ratio ( $n = 2$ ) was assessed to be  
22  
23 227  $\sim 0.08 \%$ . This result is almost a factor of 5 better than that calculated for the data reported by  
24  
25 228 Vallelonga *et al.*<sup>1</sup> (0.39 %,  $n = 7$ ) at  $10 \text{ pg g}^{-1}$  of Pb, using ID-TIMS and 10 g of snow.

26  
27 229 In figure 3, the data are presented in a three-isotope plot. The Pb isotope ratios plotted on a straight  
28  
29 230 line and are in agreement with data reported in literature.<sup>32</sup> Particularly, data lie between the natural  
30  
31 231 and the anthropogenic end-members reported by Van de Velde *et al.*,<sup>26</sup> and the actual values are  
32  
33 232 similar to those measured at the Hercules Névé for the period 1986–1994. The same authors pointed  
34  
35 233 out that the natural end-member is the result of a mixing of volcanic and crustal inputs, whereas the  
36  
37 234 anthropogenic end-member was governed by both South American and Australian industrial  
38  
39 235 emissions.

40  
41 236 Also Pb isotope ratios measured in the coastal area of East Antarctica<sup>33</sup> are included in Figure 3.  
42  
43 237 These values are closer to the anthropogenic end-member than those measured on the Plateau,  
44  
45 238 possibly indicating a larger anthropogenic input for the coastal area.

46  
47 239 The time-series obtained for the years 2006 and 2010 are reported in figure 4. The first year showed  
48  
49 240 a strong seasonal variation of the  $^{208}\text{Pb}/^{207}\text{Pb}$  ratio, characterised by lower values from March to  
50  
51 241 July 2006, and higher values from both December 2005 to January 2006, and from September to

1  
2 242 November 2006. Particularly, the ratios measured during spring showed values similar to those of  
3  
4 243 the pelagic sediments and South Sandwich volcanic rock,<sup>26</sup> thus suggesting a predominance of  
5  
6 244 crustal Pb for this period. This result partly contradicts that reported by Burn-Nunes *et al.*,<sup>34</sup> who  
7  
8 245 found a maximum of both anthropogenic and mineral dust occurring during spring and autumn in  
9  
10 246 the late 1880s. On the other hand, Planchon *et al.*<sup>32</sup> reported evidence of close-to-radiogenic values  
11  
12 247 for the <sup>206</sup>Pb/<sup>207</sup>Pb ratio occurring in spring/summer during maxima of dust deposition, likely  
13  
14 248 originating from South America.

15  
16  
17 249 On the contrary, a clear seasonal trend was not apparent in the Pb isotope ratios recorded for the  
18  
19 250 2010 samples, showing just minor fluctuations around the average value (<sup>208</sup>Pb/<sup>207</sup>Pb = 2.435 ±  
20  
21 251 0.005). The absence of a regular seasonal pattern was also reported by other authors, suggesting that  
22  
23 252 the transport of aerosols and their deposition on the Antarctic ice sheet are complex and may vary  
24  
25 253 from year to year.<sup>26,35</sup> To improve the understanding of this variability and to highlight possible  
26  
27 254 correlation with meteorological patterns, the analysis of more years and the use of additional  
28  
29 255 chemical markers is clearly required.

#### 30 31 32 33 34 256 **4. Conclusions**

35  
36  
37  
38 257 The method developed allowed for MC-ICP-MS Pb isotopic analysis at concentrations as low as 0.5  
39  
40 258 ng mL<sup>-1</sup>, using 0.2 mL of sample solution only. The intermediate precision of the <sup>207</sup>Pb/<sup>206</sup>Pb  
41  
42 259 measurement was 0.11 ‰ RSD (*n* = 73) and 0.31 ‰ RSD (*n* = 3) at 10 ng mL<sup>-1</sup> and 0.5 ng mL<sup>-1</sup>,  
43  
44 260 respectively.

45  
46  
47 261 The small sample consumption allowed us to combine the method with a simple analyte pre-  
48  
49 262 concentration procedure consisting of freeze-drying of 20 g samples of snow, thus providing  
50  
51 263 accurate ratios at Pb concentration levels down to 5 pg g<sup>-1</sup>. The mean concentration of the blanks  
52  
53 264 (0.5 ± 0.3 pg g<sup>-1</sup>) was sufficiently low to obtain reliable Pb isotope ratios in this range of  
54  
55 265 concentrations. Particularly, at 5 pg g<sup>-1</sup>, the uncertainty associated to the blank subtraction  
56  
57  
58  
59  
60

1  
2 266 accounted for about 38 % of the total uncertainty budget, thus still not representing the major  
3  
4 267 contribution.

5  
6 268 The analytical protocol developed was applied to the measurement of Pb isotope ratios in recent  
7  
8 269 snow samples collected at Dome C (Antarctic Plateau) during the 2006 and 2010 campaigns. These  
9  
10 270 are the first data of Pb isotope ratios measured in the Antarctic snow using MC-ICP-MS. The  
11  
12 271 relative uncertainty of the ratios measured at 5 pg g<sup>-1</sup> turned out to be competitive with that reported  
13  
14 272 in literature for ID-TIMS. Moreover, the data provided some preliminary insights into the complex  
15  
16 273 pattern of the transport of Pb towards Antarctica and its deposition on the ice sheet.  
17  
18  
19

#### 20 21 274 **Acknowledgement** 22 23

24  
25 275 This study was partially funded by the Italian National Program for Research in Antarctica (Project  
26  
27 276 2013/AZ3.04). Thanks to Harry Vandepuit for his assistance with the hardware and Dr. Paolo  
28  
29 277 Grigioni for the help with meteorological data.  
30  
31  
32  
33  
34  
35  
36  
37  
38  
39  
40  
41  
42  
43  
44  
45  
46  
47  
48  
49  
50  
51  
52  
53  
54  
55  
56  
57  
58  
59  
60

Table 1: Thermo Scientific Neptune instrument settings and data acquisition parameters.

<i>Instrumental parameters</i>	
Sample uptake rate ( $\mu\text{L min}^{-1}$ )	20
Plasma gas flow rate ( $\text{L min}^{-1}$ )	15
Auxiliary gas flow rate ( $\text{L min}^{-1}$ )	0.90
Nebuliser gas flow rate ( $\text{L min}^{-1}$ )	0.72
Sheating gas flow rate ( $\text{L min}^{-1}$ ) <sup>a</sup>	0.35
Temperature of the chamber ( $^{\circ}\text{C}$ ) <sup>a</sup>	150
RF power (W)	1200
Sampling cone	Ni; 1.1 mm $\varnothing$ orifice
Skimmer	Ni; H-type; 0.8 mm $\varnothing$ orifice
Lens settings	Optimised for maximum Pb signal intensity
Resolution mode	Low
<i>Data acquisition parameters</i>	
Scan type	Static; multi-collection
Number of blocks	7
Number of cycle/blocks	6
Integration time (s)	8.4
Magnet settling time (s)	0
Idle time (s)	3
Cup configuration <sup>b</sup>	L3: $^{202}\text{Hg}$ ; L2: $^{203}\text{Tl}$ ; L1: $^{204}\text{Pb}$ , $^{204}\text{Hg}$ ; C: $^{205}\text{Tl}$ ; H1: $^{206}\text{Pb}$ ; H2: $^{207}\text{Pb}$ ; H3: $^{208}\text{Pb}$
Resistivity of the pre-amplifier	C, L1, L2, L3: $10^{11} \Omega$ ; H1, H2, H3: $10^{12} \Omega$

<sup>a</sup> Parameters of the TISIS chamber.

<sup>b</sup> As a result of the low isotopic abundance of  $^{204}\text{Pb}$  and the spectral overlap from  $^{204}\text{Hg}$ , Pb isotope ratios including this Pb isotope were not considered.

1  
2  
3  
4  
5  
6  
7  
8  
9  
10  
11  
12  
13  
14  
15  
16  
17  
18  
19  
20  
21  
22  
23  
24  
25  
26  
27  
28  
29  
30  
31  
32  
33  
34  
35  
36  
37  
38  
39  
40  
41  
42  
43  
44  
45  
46  
47  
48  
49  
50  
51  
52  
53  
54  
55  
56  
57  
58  
59  
60

Table 2: Lead isotope ratios measured in the snow collected at Dome C in the 2006 and 2010 campaigns. Uncertainties are reported as  $\pm 95$  % confidence interval.

Date	Pb (ng)	$^{207}\text{Pb}/^{206}\text{Pb}$	U	$^{208}\text{Pb}/^{206}\text{Pb}$	U	$^{208}\text{Pb}/^{207}\text{Pb}$	U
<i>2006</i>							
Dec-05	2.5	0.8650	0.0002	2.1048	0.0006	2.4333	0.0008
Jan-06	0.2	0.8630	0.0010	2.0984	0.0016	2.4317	0.0014
Feb-06	–	–	–	–	–	–	–
Mar-06	0.5	0.8685	0.0002	2.1057	0.0005	2.4244	0.0004
Apr-06	0.5	0.8747	0.0002	2.1160	0.0005	2.4190	0.0004
May-06	0.8	0.8700	0.0002	2.1082	0.0005	2.4233	0.0004
Jun-06	0.5	0.8691	0.0002	2.1070	0.0005	2.4242	0.0004
Jul-06	0.4	0.8629	0.0002	2.1020	0.0008	2.4360	0.0007
Aug-06	0.2	0.8455	0.0011	2.0727	0.0016	2.4513	0.0017
Sep-06	0.3	0.8542	0.0004	2.0914	0.0007	2.4484	0.0006
Oct-06	1.1	0.8445	0.0002	2.0692	0.0005	2.4503	0.0005
Nov-06	0.1	0.8469	0.0009	2.0774	0.0014	2.4529	0.0013
Dec-06	–	–	–	–	–	–	–
<i>2010</i>							
Jan-10	0.2	0.8616	0.0020	2.0971	0.0035	2.4340	0.0025
Feb-10	2.0	0.8661	0.0002	2.1046	0.0004	2.4299	0.0004
Mar-10	1.4	0.8626	0.0002	2.0979	0.0004	2.4321	0.0003
Apr-10	1.0	0.8650	0.0002	2.1041	0.0004	2.4324	0.0003
May-10	14	0.8701	0.0002	2.1108	0.0006	2.4259	0.0007
Jun-10	0.4	0.8596	0.0002	2.0939	0.0005	2.4358	0.0005
Jul-10	0.6	0.8596	0.0003	2.0945	0.0006	2.4367	0.0007
Aug-10	0.2	0.8606	0.0004	2.0969	0.0008	2.4364	0.0008
Sep-10	1.3	0.8640	0.0005	2.1006	0.0008	2.4312	0.0012
Oct-10	0.3	0.8591	0.0004	2.0956	0.0007	2.4393	0.0007
Nov-10	0.1	0.8499	0.0005	2.0799	0.0014	2.4473	0.0019
Dec-10	0.4	0.8608	0.0002	2.0974	0.0006	2.4365	0.0006

1  
2  
3  
4  
5  
6  
7  
8  
9  
10  
11  
12  
13  
14  
15  
16  
17  
18  
19  
20  
21  
22  
23  
24  
25  
26  
27  
28  
29  
30  
31  
32  
33  
34  
35  
36  
37  
38  
39  
40  
41  
42  
43  
44  
45  
46  
47  
48  
49  
50  
51  
52  
53  
54  
55  
56  
57  
58  
59  
60

*Figure 1:* Variation of the  $^{207}\text{Pb}/^{206}\text{Pb}$  isotope ratio repeatability (internal precision) with the Pb concentration. The solid line is the best-fitting curve through the experimental data and the error bars represent the standard deviation of the average repeatability ( $n = 3$ ).

1  
2  
3  
4  
5  
6  
7  
8  
9  
10  
11  
12  
13  
14  
15  
16  
17  
18  
19  
20  
21  
22  
23  
24  
25  
26  
27  
28  
29  
30  
31  
32  
33  
34  
35  
36  
37  
38  
39  
40  
41  
42  
43  
44  
45  
46  
47  
48  
49  
50  
51  
52  
53  
54  
55  
56  
57  
58  
59  
60

*Figure 2:* Contribution to the combined uncertainty of the measurement precision for the Pb isotope ratio in the sample ( $r_x$ ); the measurement precision for the Tl isotope ratio ( $r_s$ ); the uncertainty associated to the certified value for NIST SRM 981 ( $R_c$ ), and the blank ( $r_b$ ). In sub-figures (a), (b) and (c) samples with a Pb concentration of 5, 23 and 700  $\text{pg g}^{-1}$  are considered.

1  
2  
3  
4  
5  
6  
7  
8  
9  
10  
11  
12  
13  
14  
15  
16  
17  
18  
19  
20  
21  
22  
23  
24  
25  
26  
27  
28  
29  
30  
31  
32  
33  
34  
35  
36  
37  
38  
39  
40  
41  
42  
43  
44  
45  
46  
47  
48  
49  
50  
51  
52  
53  
54  
55  
56  
57  
58  
59  
60

*Figure 3:* three-isotopes plot showing the results obtained for the Antarctic snow samples collected at Dome C during the 2006 (●) and 2010 (●) campaigns, respectively. For comparison, data from Bazzano *et al.*<sup>33</sup> determined in particulate matter from Terra Nova Bay (Coastal Antarctica) are also reported (○), while the shaded areas are from Van de Velde *et al.*<sup>26</sup>. All the error bars represent 95 % confidence intervals.

1  
2  
3  
4  
5  
6  
7  
8  
9  
10  
11  
12  
13  
14  
15  
16  
17  
18  
19  
20  
21  
22  
23  
24  
25  
26  
27  
28  
29  
30  
31  
32  
33  
34  
35  
36  
37  
38  
39  
40  
41  
42  
43  
44  
45  
46  
47  
48  
49  
50  
51  
52  
53  
54  
55  
56  
57  
58  
59  
60

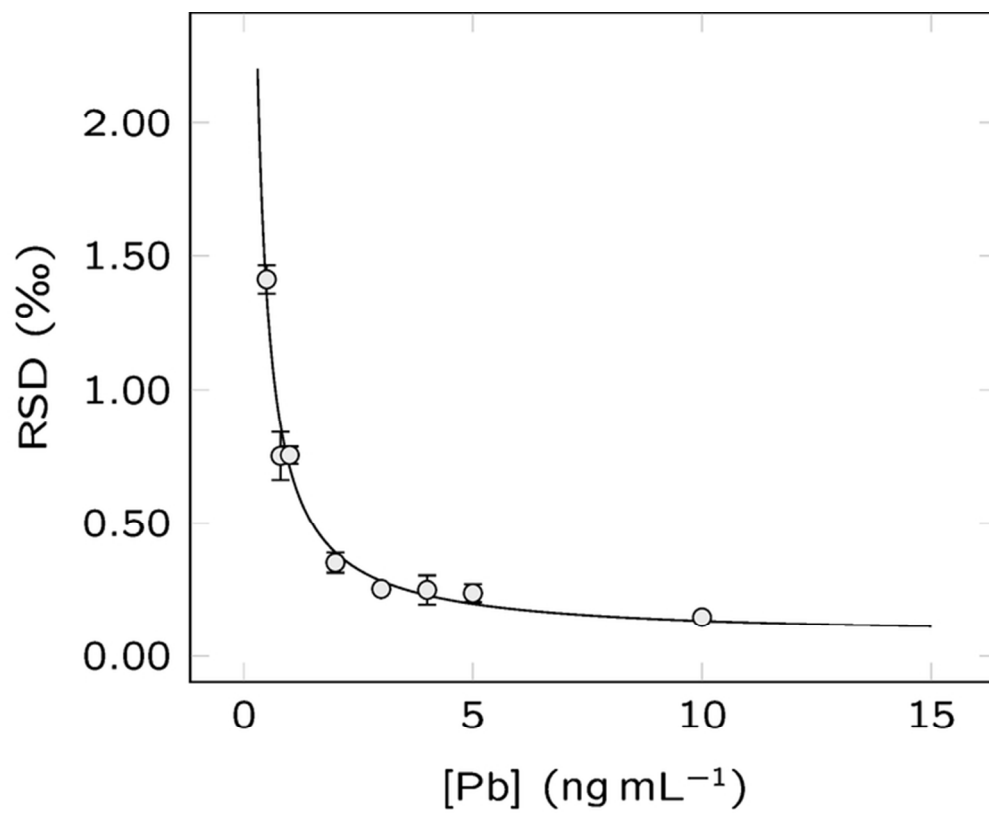
*Figure 4:* annual variation of the  $^{208}\text{Pb}/^{207}\text{Pb}$  ratio for both the periods considered. Error bars represent 95% confidence intervals.

## References

- 1  
2  
3  
4 278 1 P. Vallelonga, P. Gabrielli, E. Balliana, A. Wegner, B. Delmonte, C. Turetta, G. Burton, F.  
5  
6 279 Vanhaecke, K. J. R. Rosman, S. Hong, C. F. Boutron, P. Cescon and C. Barbante, *Quat. Sci.*  
7  
8  
9 280 *Rev.*, 2010, 29, 247–255.  
10  
11  
12 281 2 P. Vallelonga, P. Gabrielli, K. J. R. Rosman, C. Barbante and C. F. Boutron, *Geophys. Res.*  
13  
14 282 *Lett.*, 2005, 32, 1–4.  
15  
16  
17 283 3 K. J. R. Rosman, W. Chisholm, C. F. Boutron, J.-P. Candelone, J.-L. Jaffrezo and C. I.  
18  
19 284 Davidson, *Earth Planet. Sci. Lett.*, 1998, 160, 383–389.  
20  
21  
22  
23 285 4 K. J. R. Rosman, W. Chisholm, C. F. Boutron, J.-P. Candelone and C. C. Patterson, *Geophys.*  
24  
25 286 *Res. Lett.*, 1994, 21, 2669–2672.  
26  
27  
28  
29 287 5 W. Chisholm, K. J. R. Rosman, C. F. Boutron, J. P. Candelone and S. Hong, *Anal. Chim.*  
30  
31 288 *Acta*, 1995, 311, 141–151.  
32  
33  
34 289 6 P. Vallelonga, K. Van de Velde, J. P. Candelone, C. Ly, K. J. R. Rosman, C. F. Boutron, V. I.  
35  
36 290 Morgan and D. J. Mackey, *Anal. Chim. Acta*, 2002, 453, 1–12.  
37  
38  
39  
40 291 7 L. Balcaen, L. Moens and F. Vanhaecke, *Spectrochim. Acta, Part B*, 2010, 65, 769–786.  
41  
42  
43 292 8 J. L. Todoli and J. M. Mermet, *J. Anal. At. Spectrom.*, 2002, 17, 913–921.  
44  
45  
46 293 9 J.-L. Todoli and J.-M. Mermet, *J. Anal. At. Spectrom.*, 2002, 17, 345–351.  
47  
48  
49  
50 294 10 C. Lagomarsino, M. Grotti, J. L. Todoli and J. M. Mermet, *J. Anal. At. Spectrom.*, 2007, 22,  
51  
52 295 523.  
53  
54  
55  
56  
57  
58  
59  
60

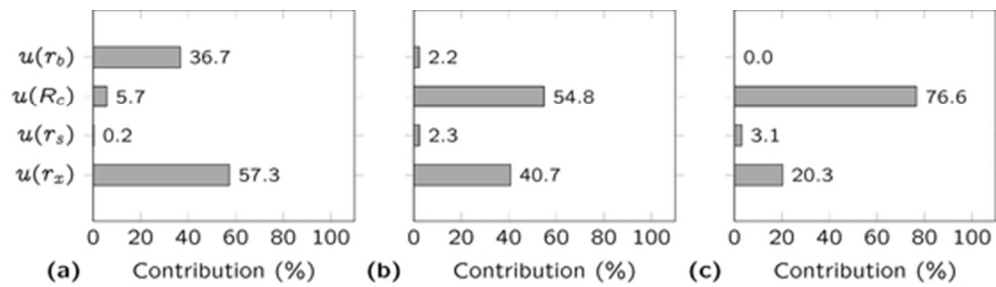
- 1  
2 296 11 F. Ardini, M. Grotti, R. Sánchez and J. L. Todolí, *J. Anal. At. Spectrom.*, 2012, 27, 1400–  
3  
4 297 1404.  
5  
6  
7 298 12 M. Grotti, F. Ardini and J. L. Todoli, *Anal. Chim. Acta*, 2013, 767, 14–20.  
8  
9  
10 299 13 E. Paredes, M. Grotti, J. M. Mermet and J. L. Todolí, *J. Anal. At. Spectrom.*, 2009, 24, 903.  
11  
12  
13 300 14 E. Paredes, D. G. Asfaha, E. Ponzevera, C. Brach-Papa, M. Van Bocxstaele, J. L. Todoli and  
14  
15 301 C.R. Quétel, *J. Anal. At. Spectrom.*, 2011, 26, 1372–1379.  
16  
17  
18 302 15 E. Paredes, D. G. Asfaha and C. R. Quétel, *J. Anal. At. Spectrom.*, 2013, 28, 320–326.  
19  
20  
21 303 16 E. Paredes, J. L. Todoli and C. R. Quétel, *J. Anal. At. Spectrom.*, 2013, 28, 327–333.  
22  
23  
24 304 17 A. Bazzano and M. Grotti, *J. Anal. At. Spectrom.*, 2014, 29, 926–933.  
25  
26  
27 305 18 J. Woodhead, *J. Anal. At. Spectrom.*, 2002, 17, 1381–1385.  
28  
29  
30 306 19 D. C. Baxter, I. Rodushkin, E. Engström and D. Malinovsky, *J. Anal. At. Spectrom.*, 2006,  
31  
32 307 21, 427.  
33  
34  
35 308 20 M. Grotti, F. Soggia and J. Luis Todoli, *Analyst*, 2008, 133, 1388–94.  
36  
37  
38 309 21 A. Cocherie and M. Robert, *Chem. Geol.*, 2007, 243, 90–104.  
39  
40  
41 310 22 T. Kuritani and E. Nakamura, *Chem. Geol.*, 2002, 186, 31–43.  
42  
43  
44 311 23 Y. Amelin and W. J. Davis, *J. Anal. At. Spectrom.*, 2006, 21, 1053.  
45  
46  
47 312 24 A. Makishima and E. Nakamura, *J. Anal. At. Spectrom.*, 2010, 25, 1712.  
48  
49  
50 313 25 M. F. Thirlwall, *Chem. Geol.*, 2002, 184, 255–279.  
51  
52  
53  
54  
55  
56  
57  
58  
59  
60

- 1  
2 314 26 K. Van de Velde, P. Vallelonga, J.-P. Candelone, K. J. R. Rosman, V. Gaspari, G. Cozzi, C.  
3  
4 315 Barbante, R. Udisti, P. Cescon and C. F. Boutron, *Earth Planet. Sc. Lett.*, 2005, 232, 95–108.  
5  
6  
7 316 27 BIPM, IEC, IFCC, ISO, IUPAC, IUPAP and OIML, *Guide to the expression of uncertainty in*  
8  
9 317 *measurement*, 2nd edn., 1995.  
10  
11  
12 318 28 R. N. Taylor, O. Ishizuka, A. Michalik, J. A. Milton and I. W. Croudace, *J. Anal. At.*  
13  
14 319 *Spectrom.*, 2014, 30, 198–213.  
15  
16  
17 320 29 J. Baker, D. Peate, T. Waight and C. Meyzen, *Chem. Geol.*, 2004, 211, 275–303.  
18  
19  
20 321 30 M. Grotti, F. Soggia, F. Ardini, E. Magi, S. Becagli, R. Traversi and R. Udisti, *Chemosphere*,  
21  
22 322 2015, *in press*. DOI 10.1016/j.chemosphere.2014.10.094  
23  
24  
25 323 31 R. Udisti, S. Becagli, S. Benassai, E. Castellano, I. Fattori, M. Innocenti, A. Migliori and R.  
26  
27 324 Traversi, *Ann. Glaciol.*, 2004, 39, 53–61.  
28  
29  
30 325 32 F. A. M. Planchon, K. van de Velde, K. J. R. Rosman, E. W. Wolff, C. P. Ferrari and C. F.  
31  
32 326 Boutron, *Geochim. Cosmochim. Acta*, 2003, 67, 693–708.  
33  
34  
35 327 33 A. Bazzano, F. Soggia and M. Grotti, *Environ. Chem.*, 2015, *in press*. DOI  
36  
37 328 10.1071/EN14185.  
38  
39  
40 329 34 L. J. Burn-Nunes, P. Vallelonga, R. D. Loss, G. R. Burton, A. Moy, M. Curran, S. Hong, A.  
41  
42 330 M. Smith, R. Edwards, V. I. Morgan and K. J. R. Rosman, *Geochim. Cosmochim. Acta*,  
43  
44 331 2011, 75, 1–20.  
45  
46  
47 332 35 F. A. M. Planchon, C. F. Boutron, C. Barbante, G. Cozzi, V. Gaspari, E. W. Wolff, C. P.  
48  
49 333 Ferrari and P. Cescon, *Sci. Total Environ.*, 2002, 300, 129–142.  
50  
51  
52  
53  
54  
55  
56  
57  
58  
59  
60

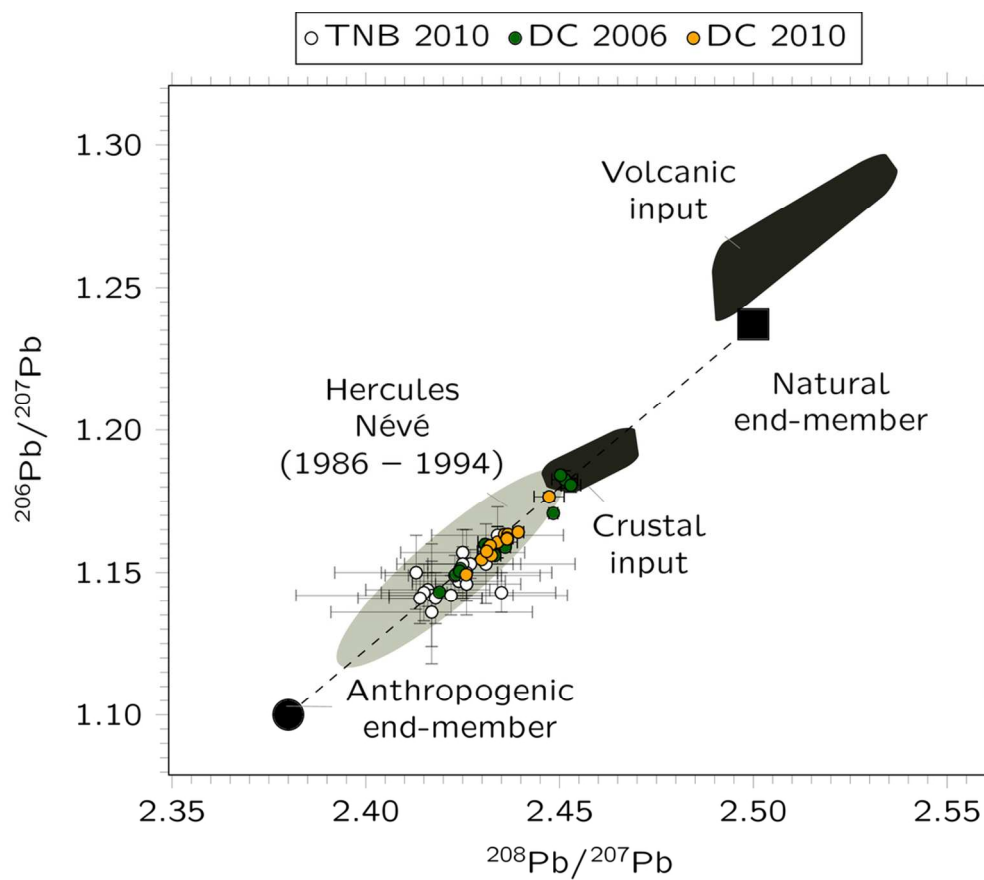


64x52mm (300 x 300 DPI)

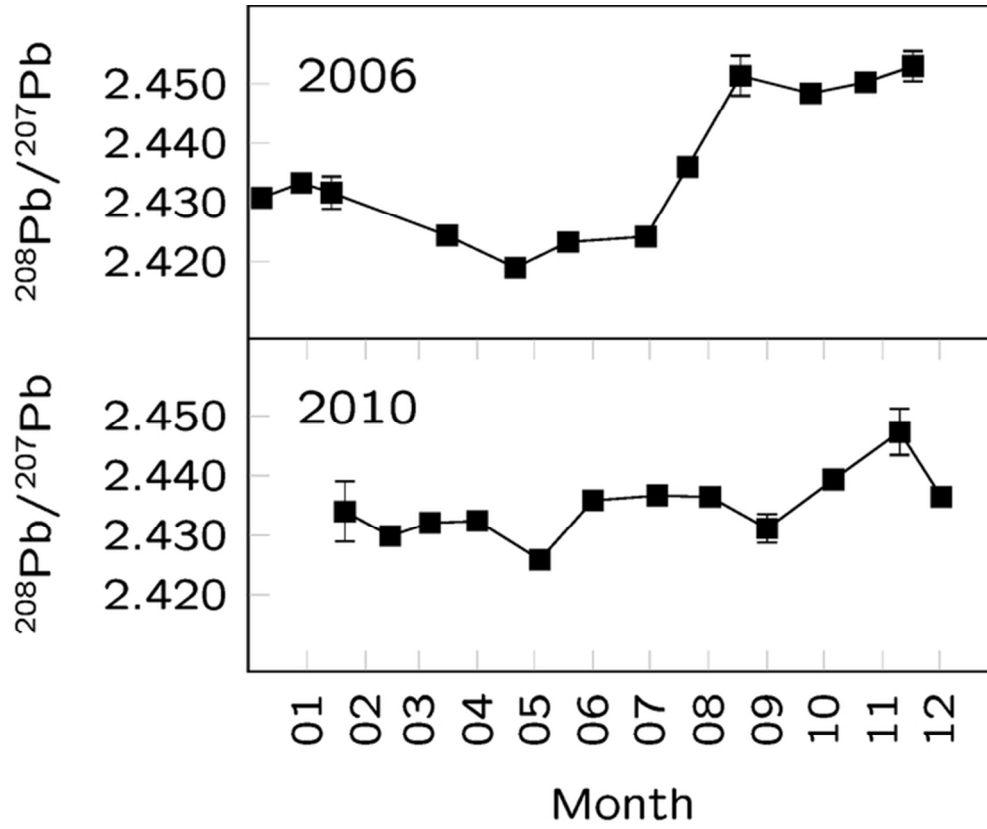
1  
2  
3  
4  
5  
6  
7  
8  
9  
10  
11  
12  
13  
14  
15  
16  
17  
18  
19  
20  
21  
22  
23  
24  
25  
26  
27  
28  
29  
30  
31  
32  
33  
34  
35  
36  
37  
38  
39  
40  
41  
42  
43  
44  
45  
46  
47  
48  
49  
50  
51  
52  
53  
54  
55  
56  
57  
58  
59  
60



47x13mm (300 x 300 DPI)



101x88mm (300 x 300 DPI)



60x50mm (300 x 300 DPI)

1  
2  
3  
4  
5  
6  
7  
8  
9  
10  
11  
12  
13  
14  
15  
16  
17  
18  
19  
20  
21  
22  
23  
24  
25  
26  
27  
28  
29  
30  
31  
32  
33  
34  
35  
36  
37  
38  
39  
40  
41  
42  
43  
44  
45  
46  
47  
48  
49  
50  
51  
52  
53  
54  
55  
56  
57  
58  
59  
60